Insertion Reaction of Mn⁺ Bare Metal Cation into the N−H and C−H Bonds of Ammonia and Methane

Maria del Carmen Michelini, Nino Russo,* and Emilia Sicilia

Dipartimento di Chimica and Centro di Calcolo ad Alte Prestazioni per Elaborazioni Parallele e Distribuite-Centro d'Eccellenza MURST, Università della Calabria, I-87030 Arcavacata di Rende, Italy
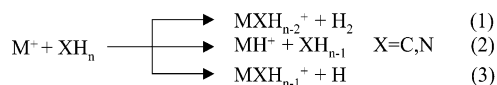
The Potential Energy Surfaces of the dehydrogenation reaction of NH_3 and CH_4 molecules by the first-row transition metal cations Mn⁺ (^7S, ^5S) were investigated employing the Density Functional (B3LYP) and the CCSD(T) levels of theory. A close description of the reaction paths leading to three dissociation products was given, including several minima and key transition states. The reactions proceed to give dehydrogenation products by oxidative addition of the metal cation into one of the H−X bonds (X = N,C) and formation of the H−M⁺−XH_{n−1}, hydrido intermediates, which in these cases are also confirmed to represent stable minima along the quintet surface. Because the spin state of the reactants is different from that of intermediates and products an intersystem crossing is proposed to occur. The binding energies of reaction products were calculated and compared with available experimental data to calibrate the quality of our approach.

1. Introduction

Gas-phase study of the reactions of transition metal ions with small molecules containing prototypical bonds (e.g., C−H, C−C, N−H, O−H) is an active area of interest in chemistry because of their importance in catalytic research.[1−26] Indeed, among the useful approaches, gas-phase experiments provide the opportunity to obtain valuable information on elementary reactions and mechanisms in a controlled environment, without disturbing factors, such as the presence of other ligands, counterions, and solvent molecules. In this field, guided ion-beam mass spectrometry was used extensively to study ion–molecule reactions, providing a considerable amount of information on the catalytic activity of transition metal cations.[1−26] However, from an experimental point of view, explicit information on all of the elementary steps involved along the whole reaction path is often difficult to obtain, and a closer interaction between theory and experiment has turned out to be very fruitful in this area of chemistry.[27−33] Moreover, the availability of experimental data concerning the activation reactions of small molecules by transition metals makes possible to check the reliability of quantum chemical tools in the description of these processes. On the other hand, the disagreement between theory and experiment can encourage more accurate experimental investigations and improve of the theoretical approaches.

Experimentally, it was shown that the following reactions can be detected during the interaction of first-row transition cations, M⁺, with ammonia and methane

$$M^+ + XH_n \longrightarrow \begin{cases} MXH_{n-2}^+ + H_2 & (1) \\ MH^+ + XH_{n-1} \quad X=C,N & (2) \\ MXH_{n-1}^+ + H & (3) \end{cases}$$

with branching ratios that vary across the periodic table. For early and middle metals, the H_2 elimination process is the most thermodynamically favored, whereas at higher energies, the

other reaction products become accessible.[5,7−9,15,18,19] The mechanism proposed for these reactions implies an oxidative addition of the metal cation into one of H−X (X = N, C) bonds to form a hydrido intermediate that may lie either lower or higher in energy than the reactants and is believed to constitute a minimum along the potential energy surface (PES). The differences found in the measured strengths of the M−N bonds with respect to the carbon analogues were attributed to the presence of a lone pair on the nitrogen atom of ammonia ligand. The N atom has the same number of valence electrons with the same orbital hybridization of carbon in methane.[34]

Another topic of interest in these reactions is the ability of the metal center to access multiple low-lying electronic states and to adapt to different bonding situations, which may enable the system to find low-energy reaction paths not accessible otherwise. This kind of behavior, in which more than one spin surface connects the reactants and products, is generally referred to as two-state reactivity (TSR)[35] and was proposed to play a fundamental role in organometallic chemistry.

This paper is a continuation of two previous Density Functional (DF) studies concerning the reaction of Sc−Cr series of cations with ammonia and methane[32,33] and gives a detailed information about the potential energy surfaces for the activation reactions of N−H and C−H bonds by Mn⁺. On the contrary to the cases examined previously, no detailed experimental information on the mechanism and the energetics of the Mn⁺ activation reactions of ammonia and methane is available in the literature. Moreover, Mn-containing species are also a challenge for theoretical computations because, due to the large number of unpaired electrons, correlation effects are critically important. Then, besides DF computations, the reaction paths were also described by using the coupled-cluster approximation,[36,37] which represents one of the most accurate ab initio methods available at the present time and is considered reliable to treat open-shell transition metal containing systems.[38−42]

On the basis of the electronic state dependence of Mn⁺ reactions evidenced by ion cyclotron resonance experiments,[43] Strobel and Ridge proposed qualitative PES involved in the

---

reaction of the Mn^+ ion with ammonia. The mechanism of the reaction of manganese ion with $R-CH_3$ molecules was discussed as a result of a mass-spectrometric study in which the electronic state of the ion was varied.[44] Gas-phase first-row transition metal ions, from Sc^+ to Zn^+ (reactions with small alkanes including methane), were studied in a multicollisional environment.[10] In this context, an intersection between the potential surfaces was hypothesized. Finally, bond dissociation energies (BDEs) of M^+-NH_3 complexes of first-row transition metals were determined examining their collision-induced dissociation reactions.[45]

On the theoretical side, the CASSCF method combined with gradient techniques was used to study the stability of the low-spin hydridomethyl complexes, $HMCH_3^+$, of the first-row transition metal cations.[46] Geometries, electronic structures, and binding energies of these species, corresponding to stable intermediates in the insertion reactions into the $C-H$ bond, were reported together with those of the transition states leading to them. The properties of the adducts formed upon interaction of ammonia with the ions of interest were calculated by using a modified extended Huckel molecular orbital model,[47] and their binding energies were also determined using the modified coupled-pair functional approach.[48]

Recently, Ugalde et al. have systematically studied the dehydrogenation mechanism of water by the first-row transition metal ions,[27−30] so a useful comparison between their results and ours can highlight the influence of different ligands on the reactivity of the same metal center.

2. Method

The Density Functional (DF) theory in its three-parameter hybrid B3LYP[49,50] formulation was the computational method used for geometry optimization and frequency calculations together with the DZVP (for the transition metal) and TZVP (for the other atoms) sets given by Godbout et al.[51] The choice of the B3LYP DF method was motivated by its satisfactory performance in describing transition metal containing systems even for complex situation such as those present in open-shell transition metal compounds.[39,52,53] Moreover, previous works on this subject[27−30,40,52−54] proven that DF theory, for transition metal cation containing systems, is successful in determining geometries that are reliable and comparable to those obtained with highly correlated methods, at a significantly lower computational cost. The TZVP+G(3df,2p) basis set, previously used by Ugalde et al.[29] for the metal, was also employed for DF computations to establish whether a larger basis set would influence significantly the quantitative behavior of the PES's. Single point B3LYP/TZVP+G(3df,2p) calculations were carried out at the B3LYP/DZVP equilibrium geometries.

For each optimized stationary point vibrational analysis was performed to determine its minimum or saddle point character and to evaluate the zero-point vibrational energy (ZPE) corrections, which are included in all relative energies.

To gauge the B3LYP results on the stationary points, single point computations were performed using the coupled cluster method including single, double, and perturbative treatment of triple excitations (CCSD(T)).[36,37] The optimized geometries and the ZPE from the corresponding B3LYP/DZVP computations were used in conjunction with the above-mentioned TZVP+G-(3df,2p) basis set. In these CCSD(T) computations, the 1s electrons of C and N and 1s to 2p electrons of Mn were not correlated. For the sake of clarity, the B3LYP/TZVP+G(3df,-2p)//B3LYP/DZVP and CCSD(T)/TZVP+G(3df,2p)//B3LYP/DZVP computations will be referred to as B3LYP/TZVP and CCSD(T)/TZVP in the following sections.

TABLE 1: Relative Energies of the ^5S (sd^5) Excited State of Mn^+ with Respect to the Ground ^7S (sd^5) State (Δ) and Metal−Ligand Bond Strengths for MnH$^+$ (BE$_1$), MnCH$_3^+$ (BE$_2$), and MnCH$_2^+$ (BE$_3$) Systems

level of theory	Δ	BE$_1$	BE$_2$	BE$_3$
B3LYP/DZVP	15.13[a]	53.3	54.5	75.5
B3LYP/TZVP	19.74[a]	49.7	50.2	69.7
CCSD(T)/TZVP	18.79[a]	40.5	42.1	54.4
exp.	26.98[b]	47.5 ± 3.5[c]	49.1 ± 0.9[e]	68.3 ± 2.1[d]

All the values are in kcal/mol. [a] Ref 29. [b] Ref 58. [c] Ref 59. [d] Ref 60, 61. [e] Ref 61.

A full Natural Bond Orbital (NBO) analysis[55,56] was performed for some stationary points along the energy paths to give further insight into their bonding properties.

All of the calculations reported here, both at B3LYP and CCSD(T) level, were carried out with the GAUSSIAN94/DFT[57] code.

3. Results and Discussion

3.1 Preliminary Studies. Previous theoretical studies[29] on the high- low-spin splitting of the Mn^+ cation show that the three levels of theory aforementioned, are able to correctly determine the ^7S (sd^5) ground state. According to experimental results,[58] the ^5S (sd^5) secondary excited state of interest lies 26.98 kcal/mol above. All of the reported values are underestimated with respect to that given by Moore,[58] being the best fit obtained at B3LYP/TZVP level of theory (see Table 1).

To check the accuracy that can be expected for the molecules under investigation from both B3LYP and CCSD(T) approaches, we have compared experimental and theoretical metal−ligand bond strengths of the reaction products MnH$^+$, MnCH$_3^+$, and MnCH$_2^+$ of the various exit channels for the interaction of the Mn^+ cation with methane. The calculated binding energies are reported in Table 1 together with the experimentally determined values.[59−61] The same kind of systems were used in the past to asses the ability of DFT and, in particular, of hybrid methods to give structural and electronic properties and binding energies with an accuracy comparable to, or better than, highly correlated ab initio methods, at a fraction of computational time.[62] Our experience confirms what is now generally accepted: to obtain reliable values of the metal−carbon bond strengths at CCSD-(T) level of theory, not in a qualitative sense, it is mandatory to use basis sets of appropriate size and to properly correlate the electrons of the atoms. Indeed, test calculations, performed by taking into account only valence electrons of involved atoms, gave misleading results. On the other hand, the computed B3LYP binding energies match well the experimental values, being the agreement at B3LYP/TZVP level of theory very satisfactory, both for strongly and less strongly bound species.

3.2 Potential Energy Surfaces. As is widely accepted,[5,7−9,15,18,19] the reaction of early and middle first-row transition metal ions with ammonia and methane (XH$_n$ (X = C, N)) is expected to form, in the first step, a stable ion-dipole complex. The next step, i.e., H−X bond breaking, takes place through the M^+ insertion into an H−X bond to form a low-spin H−M$^+$−XH$_{n-1}$ intermediate, this process being thermodynamically reasonable since the broken H−X bond energy is compensated for the energy of the H−M$^+$ and M$^+$−XH$_{n-1}$ bonds formation. The reaction, then, can proceed toward the formation of the dehydrogenation products, through a concerted four-center elimination of H$_2$, or formation of MH$^+$ and MXH$^+_{n-1}$ species, as the result of a simple cleavage of M−X and M−H bonds in the insertion intermediate.

The alternative proposed mechanism, which for the H$_2$ elimination (reaction 1), involves the formation of the insertion intermediate followed by the α-H migration to M$^+$ to form (H)$_2$−M$^+$−XH$_{n-2}$ and the reductive elimination of H$_2$, can be ruled out on the basis of thermochemical arguments. However, the ion−molecule (H$_2$)−M$^+$−XH$_{n-2}$ complex is assumed to be formed in the exit channel of the molecular hydrogen.

Because the spin state of the reactants differs from that of the products, the insertion process into the H−X bond must involve a transition between the reactants high-spin PES and the intermediate and products low-spin PES, therefore both potential energy surfaces have to be described properly.

The geometrical parameters of stationary points along the dehydrogenation pathways, for the quintet and septet states, are reported in Figure 1a and 1b, for ammonia and Figure 2a and 2b for methane, whereas their corresponding to theoretically predicted PESs are sketched in Figures 3 and 4, respectively.

The first step of the reaction of Mn$^+$ with ammonia is the exothermic formation of the ion−molecule complex (**I**) along both high- and low-spin PESs. The symmetry of the $^7A_1$ ground state is C$_{3v}$ (see Figure 1) and, as is shown in Figure 3, the stabilization energies with respect to the reactants are very similar at the three employed levels of theory. The bond dissociation energy of MnNH$_3^+$ system was experimentally[45] determined and theoretically calculated[48] and all the reported values, compared with those obtained by us, are collected in Table 2.

The computed binding energies fit the experimental determinations very well, but the evenness of the values does not give us the opportunity to distinguish between the performances of the used quantum-mechanical tools. It is worthy of mention that at the B3LYP/DZVP level, the $^5A_1$ state is a little bit more stable than the $^7A_1$ one.

The next step of the reaction is the insertion of Mn$^+$ into the N−H bond of ammonia to yield the intermediate H−Mn$^+$−NH$_2$ (**II**) through the formation of a transition state **TS1**, which corresponds to the shift of a hydrogen atom from nitrogen to the metal. We succeeded in locating the structures, which are three-center complexes, of the transition states related to this process for both the high- and low-spin states. Because the high-spin **TS1** structure lies higher in energy than the corresponding low-spin state, it is evident that this region of the potential energy surface, between the formation of (**I**) and (**II**) moieties, is crucial because of the surmised crossing between the two PESs with different electronic spin multiplicity. If the true reaction path is that which we propose here (see Figure 3), the intersystem crossing takes place at an energy below that of the high-spin reactants.

The insertion intermediate (**II**), although not observed experimentally, is a key structure for understanding the entire reaction mechanism. Indeed, for H−Mn$^+$−NH$_2$ containing covalent H−Mn and Mn−N bonds, two of the valence electrons of the metal are involved in the bonding, leading to a low-spin ground state for this species.

From the insertion intermediate (**II**), it is hypothesized that the reaction proceeds to yield the molecular hydrogen complex (H$_2$)Mn$^+$−NH (**III**) after passing through a **TS2** four-center transition state, which is high in energy at all the considered levels of theory and both for high and low spin multiplicities. The last step of the reaction, the direct formation of the dehydrogenation products from intermediate (**III**), occurs without an energy barrier. Due to the height of the barrier, which is necessary to overcome in order to generate dehydrogenation products (see Figure 3) and because the products are situated
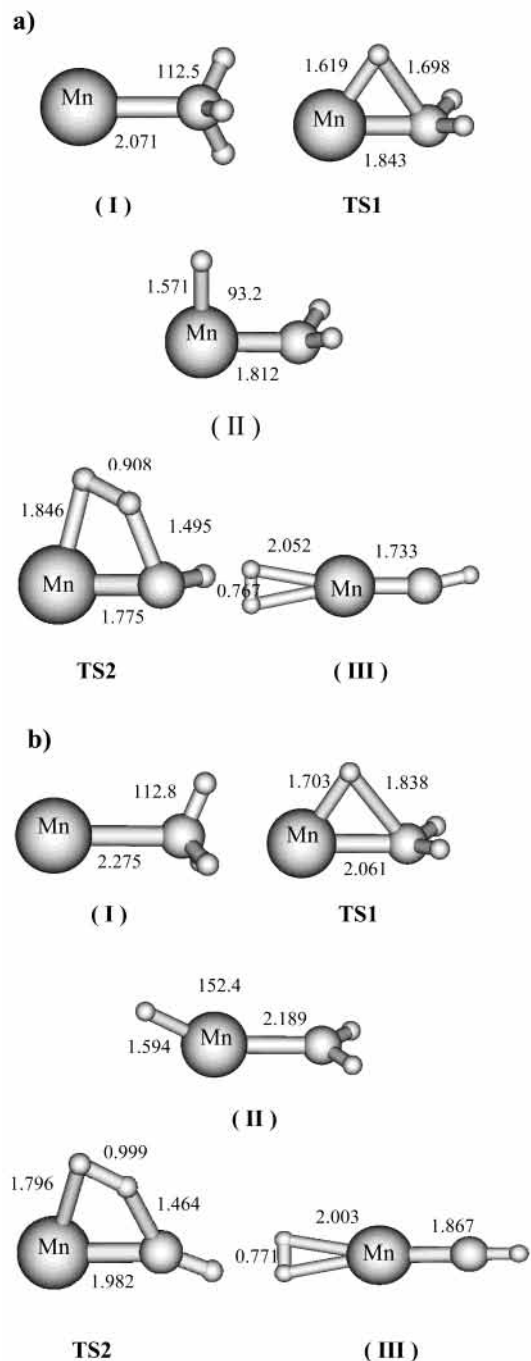

Figure 1. Geometric parameters of minima and transition states on the B3LYP/DZVP (a) quintet and (b) septet potential energy surfaces for the reaction of Mn$^+$ with NH$_3$. Bond lengths are in angstrom and angles in degrees.

well above the energy of the reactants asymptote, only the exothermic formation of the ion−dipole complex and the insertion into the N−H bond are hypothesized to occur.

For the endothermic production of MnNH$_2^+$ and MnH$^+$ species, the ground state of the products is compatible with both the high and the low-spin states of the reactants. Thus, the formation of these products would not be as sensitive to the reactant state as the dehydrogenation process. However, due to the low stability of the intermediate (**II**) in its high-spin state, it may be argued that the reaction proceeds, mainly, through the intermediate (**II**) along the low-spin potential energy surface. The reaction energy values for the formation of the MNH$_2^+$ product are only slightly higher than those relative to the
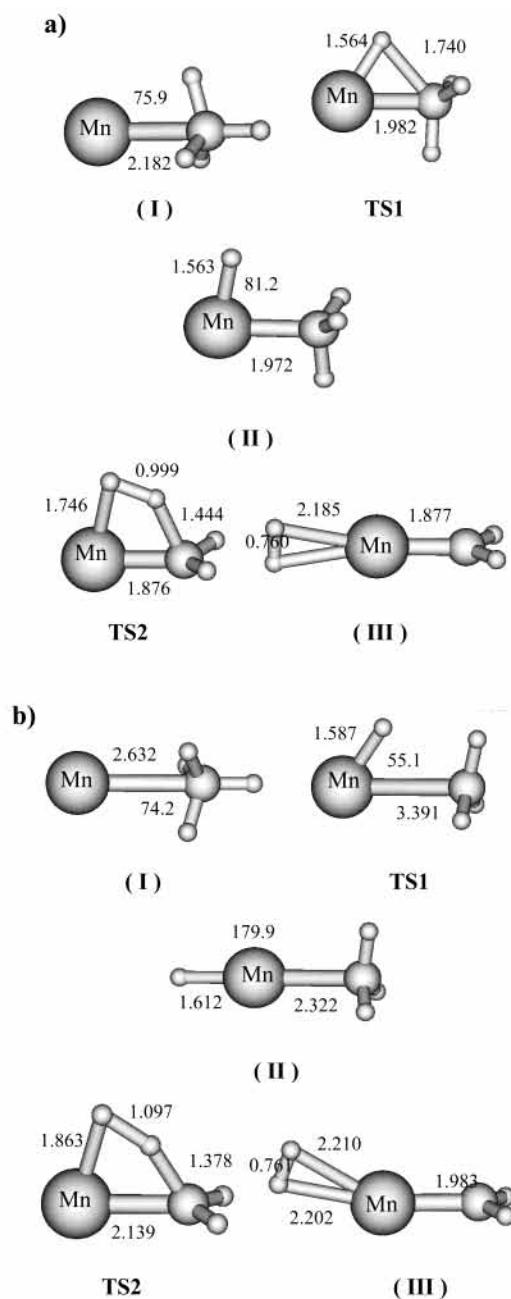
Figure 2. Geometric parameters of minima and transition states on the B3LYP/DZVP (a) quintet and (b) septet potential energy surfaces for the reaction of Mn^+ with CH_4. Bond lengths are in angstrom and angles in degrees.

dehydrogenation product and, at the CCSD(T)/TZVP level, the stability order is reversed.

Also for the reaction of manganese ion with methane the reaction paths (see Figure 4) suggest that the mechanism of the oxidative addition is operative to form the intermediate $HMnCH_3^+$. From this intermediate, the dehydrogenation reaction is predicted to be the most energetically favorable. The mechanism includes the formation, in the entrance channel, of the long-lived ion-induced-dipole complex (**I**), which subsequently yields the insertion intermediate (**II**) by migration of a hydrogen atom corresponding to the transition state **TS1**. The methane complexes (**I**) have the tridentate structures shown in Figure 2a and 2b, with C_{3v} symmetry, both in the low and high-spin states, whereas the possible bidentate structures for the same complexes are transition states, as confirmed by the vibrational analysis. At all the considered levels of theory, the formation

of the $^7A_1$ ground-state complex is exothermic, by about the same amount, with respect to the reactants in their ground state. Along the path, the ion-induced-dipole complex (**III**), (H_2)-Mn^+-CH_2, is obtained from (**II**) through the tight four-center transition state **TS2**. The difference in the ground spin state of (**I**) and (**II**) complexes is due to the hypothesized crossing between the surfaces, clearly evidenced in Figure 4. From the same figure, we can extract the information that this crossing seems to occur at an energy below that of the ground-state reactants.

Along the low-spin surface, the Mn^+ ion inserts into the C—H bond, in all cases, with a barrier in excess of reactants and leads to the quintet insertion intermediate, which is higher in energy with respect to both the Mn^+-CH_4 complex and the reactants. The relative energies of the intermediate (**II**) and the transition state leading to it, can be compared with previous CASPT2[46] computations, which give 33.1 and 45.7 kcal/mol for the intermediate and the transition state formation, respectively, with respect to the ground-state asymptote. After the formation of the $H-Mn^+-CH_3$ complex, the reaction moves toward the products conserving spin. Nevertheless, the barrier relative to the **TS2** is very high and the final step of the dehydrogenation process requires a high activation energy largely above the energy of the entrance channel. Under these circumstances, the involvement of this tight four-center transition state is highly improbable and, as a consequence, the dehydrogenation process becomes difficult.

As a consequence of the obtained results, we propose that the production of MH^+ and MCH_3^+ species occurs through metal—carbon or metal—hydrogen bonds cleavage of the intermediate (**II**) in its ground state at elevated energies.

As pointed out by Armentrout[18,19] and as confirmed by our previous computations, for the first (Sc—Ti) and the medium (Cr) cations of the row the mechanisms for the reaction with ammonia and methane are similar, although the energetics is very different. Similarities were explained considering that ammonia and methane have the same number of valence electrons with the same sp^3 hybridization of the central atom,[34] whereas differences were attributed to the presence of a lone pair on the nitrogen atom. Hence, all of the products observed in the reaction with ammonia have isoelectronic analogues to the products formed by M^+ with methane, but the M^+-NH and M^+-NH_2 product molecules have bond strengths stronger than the isoelectronic M^+-CH_2 and M^+-CH_3 species, due to the stabilization of the nitrogen lone pair. Indeed, the enhancement of the bond is a result of donation of the lone pair electrons into the empty d orbitals on the metal ion. We have not found this kind of behavior in the case of manganese. From a comparison between the PESs for the activation reactions of ammonia and methane by Mn^+ (see Figures 3 and 4) it is clear that the energy profiles are significantly different only in the region of formation of the ion—dipole complex (**I**), whereas an energy difference of a few kcal/mol was found for products formation. The absence on Mn^+ of empty d orbitals accessible to lone pair donation determines the observed different behaviors. To collect more information on this subject, we have computed B3LYP/TZVP binding energies of Mn^+-NH_2 and Mn^+-NH species that can be compared with those of Mn^+-CH_3 and Mn^+-CH_2 isoelectronic carbon analogues in Table 1. The obtained B3LYP/TZVP values are 52.6 and 53.5 kcal/mol for Mn^+-NH_2 and Mn^+-NH, respectively, which can be compared with the binding energies of the Mn^+-CH_3, Mn^+-CH_2 moieties. Although in the latter case the bond strength increases, the bond strengths of Mn^+-NH and Mn^+-NH_2 differ
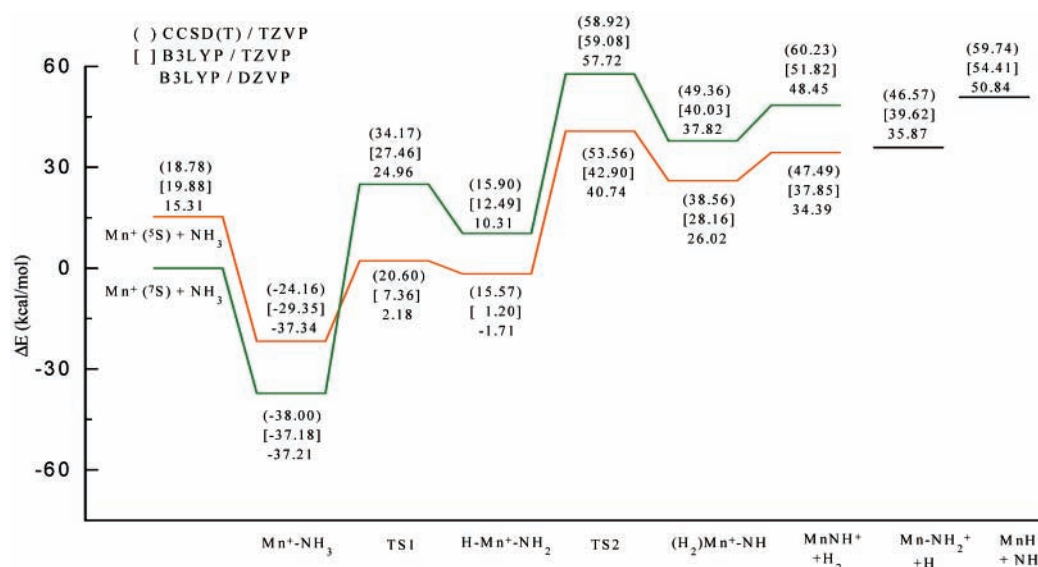
Figure 3. B3LYP/DZVP septet and quintet potential energy surfaces for the reaction of Mn+ with NH_3. B3LYP/TZVP and CCSD(T)/TZVP relative energies are reported in [ ] and ( ), respectively. Energies are in kcal/mol and relative to the ground-state reactants.

Figure 4. B3LYP/DZVP septet and quintet potential energy surfaces for the reaction of Mn+ with CH_4. B3LYP/TZVP and CCSD(T)/TZVP relative energies are reported in [ ] and ( ), respectively. Energies are in kcal/mol and relative to the ground-state reactants.
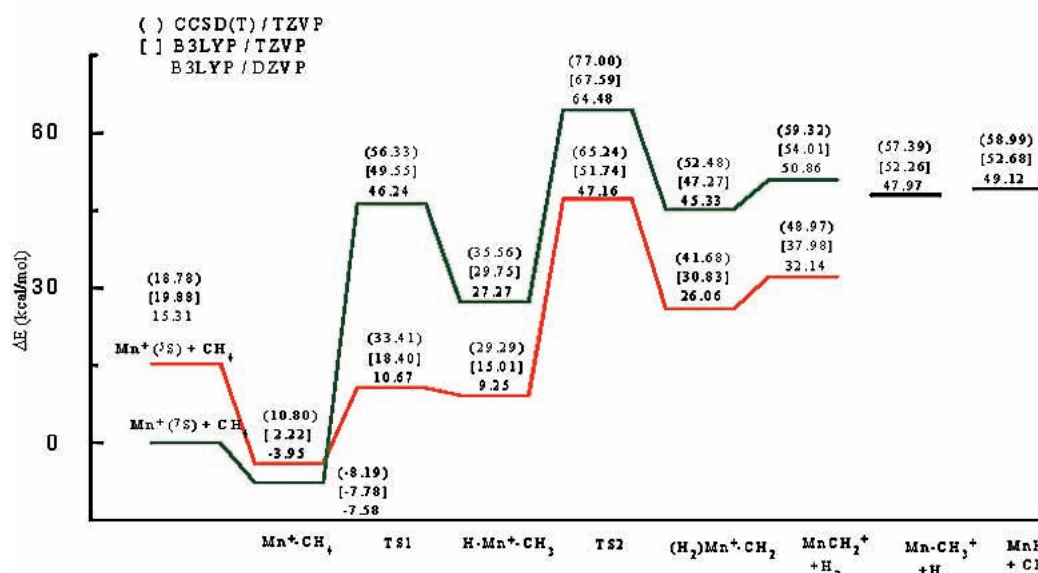
TABLE 2: Summary of 0 K Binding Energies (BE) for the $^7A_1$ $MnNH_3^+$ System

level of theory	BE
B3LYP/DZVP	37.2
B3LYP/TZVP	37.2
CCSD(T)/TZVP	38.0
MCPF/[8s,6p,4d,1f]	38.4[a]
exp.	39.0 ± 1.9[b]

All of the values are in kcal/mol. [a] Ref 48. [b] Ref 45.

slightly and are comparable to that of the MnH+ species. It is worth mentioning that in the Mn+−NH moiety, the calculated bond strength underlines the existence of a single bond. This aspect will be discussed in depth in the next section.

Although the half-filling shell of Mn+ precludes the donation from NH_3, which would reduce the stabilizing exchange energy by spin-pairing, the ammonia insertion intermediate is more stable than the methane one. The NBO analysis shows that, being the hydrogen atom partially bonded to manganese and

nitrogen, the enhanced stability of the H−Mn+−NH2 complex is due to resonance effects, which allow delocalization lowering the energy.

From a comparison between B3LYP and CCSD(T) results appears that the qualitative features of the PESs governing the mechanistic details of the X−H bond activation reactions do not show any significant difference, being the relative energetic ordering of minima and barrier heights the same. Particularly interesting is the quantitative agreement among the binding energies calculated for the high-spin ion−dipole complex (**I**) along both the surfaces for ammonia and methane activation. Overall, much larger deviations are observed among the B3LYP and CCSD(T) relative energies of stationary points along the quintet surface than those computed along the septet surface. The aforementioned (see Table 1) comparison between B3LYP and CCSD(T) binding energies against experiment of some relevant fragments for the interaction of Mn+ with methane, shows that experimental data are very well reproduced at the B3LYP level, particularly as the more extended TZVP+G(3df,-

TABLE 3: Barrier Heights (in kcal/mol) for Transition States: TS1 with Respect to Mn$^+$−NH$_3$ (Δ_1 and Δ_2), TS1 with Respect to Mn$^+$−CH$_4$ (Δ_3 and Δ_4) and TS2 with Respect to H−Mn$^+$−CH$_3$ (Δ_5)

level of theory	Δ_1(7)	Δ_2(5)	Δ_3(7)	Δ_4(5)	Δ_5(5)
B3LYP/DZVP	62.2	44.7	53.8	14.6	37.9
B3LYP/TZVP	64.6	36.7	57.3	16.2	36.7
CCSD(T)/TZVP	72.2	39.5	64.5	22.6	36.0

Multiplicities are indicated in parentheses.

2p) basis set is used, whereas some problems exist in the description of correlation energy by the applied *post*-HF approach in this case. For this reason, we believe that the B3LYP quantitative picture of the bond activation processes under examination is reliable and predictive of the real behavior of reaction paths. Finally, we would like to focus our attention on the values of the barrier heights, which for the sake of clarity are collected and compared in Table 3, along the reaction paths for the localized transition structures.

The performance of DFT approaches, and of the hybrid B3LYP functional in particular, in predicting transition states geometries and barrier heights was the subject of extensive previous works[63−67] and the general conclusion drawn for the examined classes of reactions is that Density Functional Theory based methods tend to underestimate activation barriers. Systematic studies of barrier heights along paths involving open-shell metal organic systems do not exist in the literature and the results of this work can be added to those previously obtained by Holthausen and Koch,[67] for the ethane activation by Co$^+$, to build up a broader survey of data.

3.3 Periodic Trends. Gas-phase metal−ligand bond strengths determination has become the subject of a lot of experimental and theoretical works in the past years. This interest is motivated by the importance that the knowledge of this information has in elucidating the bonding in transition-metal systems, in understanding the mechanism of a variety of catalytic reactions, in bridging the gap between ion chemistry in gas-phase and in solution. In this perspective, a useful strategy is to analyze the trends in metal−ligand binding energies resulting from the variation of the transition metal center, the ligand and the number of ligands.

We present here a comparison of bond energies, collected in the present and our previous works on this subject, of some fragments arising from the interaction of the first-row transition cation with ammonia and methane. The examined systems are the ground-states of MH$^+$, MCH$_3^+$, MCH$_2^+$, MCH$^+$, MNH$_2^+$, and MNH$^+$ for the row cations from Sc to Mn. The MCH$^+$ fragments, even if not included among the products of the studied reactions, are taken into account as a term of comparison. The binding energies calculated at B3LYP/TZVP level are reported in Figure 5 together with experimental values.[2,7−9,13,18,19,21,59−61,69−75]

The general trends of the calculated binding energies show a satisfactory agreement with the experimental values, although some pronounced discrepancies are found. It should be underlined that some experimental data are preliminary[74] and, as a consequence, deserve further experimental work to be confirmed.

Several observations are noteworthy. The calculated bond strength in hydride cations decreases from Sc to Cr and then increases for Mn. This behavior can be attributed[76,77] to the loss of exchange energy and to the required promotion energy, if the spin-pairing of 4s orbital of M$^+$ in its $4s3d^{n-1}$ configuration is considered responsible of the bond formation. The same explanation can be applied to the similar trend of single-bond
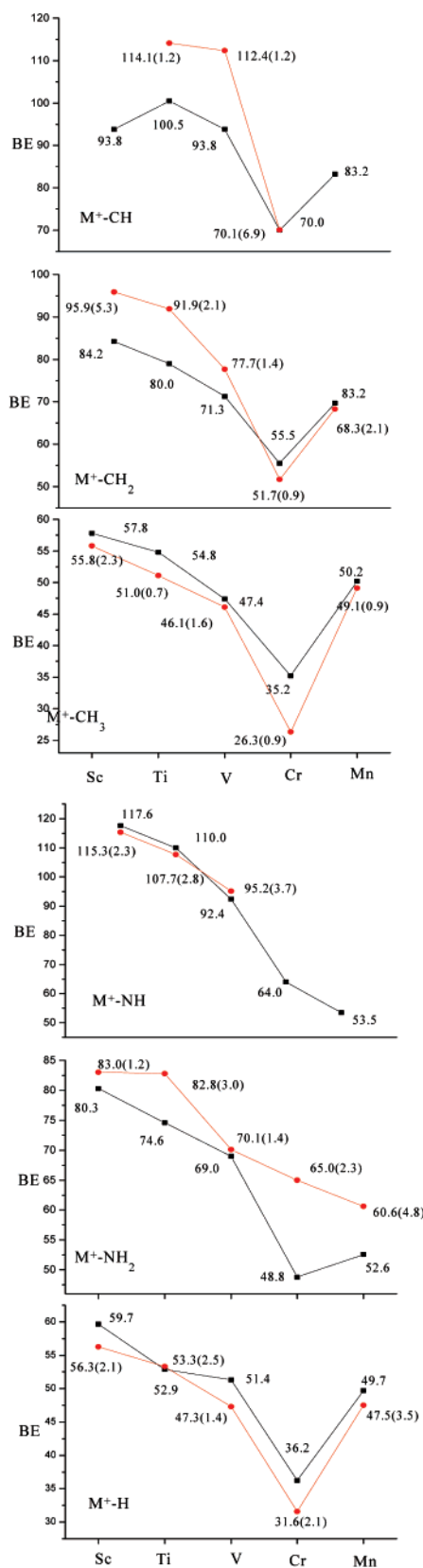

Figure 5. Calculated B3LYP/TZVP (■) and experimental (●) binding energies (BE), in kcal/mol, for the ground state of MCH$^+$, MCH$_2^+$, MCH$_3^+$, MNH$^+$, MNH$_2^+$, and MH$^+$ species from Sc$^+$ to Mn$^+$. Experimental values are taken from refs 2, 7−9, 13, 18, 19, 21, 59−61, 69−75. Experimental uncertainties are reported in parentheses.

energies of the metal-methyl systems. The M$^+$−CH$_2$ binding energies and bond lengths are consistent with the presence of a double bond formed with unpaired electrons on carbon and the

trend underlined before is conserved along the row. Also, in this case, a model which takes into account the promotion energy and the spin decoupling of the electrons involved in the bonds can be invoked[78] to account for the reported tendency. In moving across the transition elements series, a different behavior is observed for the MCH$^+$ species because scandium cannot support more than two covalent bonds, whereas triple-bond energies and lengths are exhibited by all of the other cations examined. The metal-amide ions, except for manganese, are characterized by bond strengths that are comparable to those of methylene systems and are consistent with the interpretation that the NH$_2$ group is doubly bonded to the metal, the additional bond arising from the dative interaction of nitrogen lone pair with empty metal 3d orbitals. The reduced bond strength for the amide complex of manganese, lacking in empty d orbitals, can be just given to the absence, as confirmed by NBO analysis, of the dative bond, and not to the loss of exchange energy as proposed by Kapellos et al.[79] Imido complexes have rather large binding energies which can be explained in terms of the multiple bond character between the metal and the NH moiety. Indeed, it can be assumed that a strong triple bond can be formed including again dative interaction of the nitrogen lone pair with the accessible d orbitals of the metal. An analysis of the bond reveals that the situation is different for chromium cation because of the donation of electron density from the nitrogen lone pair is partial. For this reason, the energy gain in going from a single to a double to a triple bond is reduced with respect the early cations of the row. As yet pointed out, manganese complex shows a smaller binding energy according to the presence of a single σ bond formed with one unpaired electron on the sp^2 hybridized nitrogen atom of the NH group (the bond angle is 134°) and the lone pair occupying the p orbital. All of the linear structures for the same species localized along the path are transition states, as confirmed by the vibrational analysis.

4. Conclusions

The results of this study on the interaction of Mn$^+$ with ammonia and methane indicate that the most likely reaction mechanism proceeds via oxidative addition of a H−X (X = N, C) bond to yield the H−Mn−XH$_{n-1}$ intermediate. A simple bond cleavage forms MnH$^+$ and MnXH$^+_{n-1}$ in endothermic processes, whereas the molecular elimination of H$_2$ leads to the formation, also in this case endothermic, of dehydrogenation products. Potential energy surfaces were investigated in detail at the B3LYP/DZVP level of theory, considering both the low (quintet) and the high-spin (septet) states of the cation. Single point calculations at the optimized geometries were carried out by using a more extended TZVP+G(3df,2p) basis set and at CCSD(T) level of theory, employing the same triple-ζ quality basis set. The qualitative picture of the PESs does not change, but the quantitative agreement with available experimental data is improved when the quality of the basis set is increased, at B3LYP level. The main features of the surfaces are preserved, also with respect to CCSD(T), but some larger differences are observed among relative energies of stationary points, particularly along the quintet path.

The key reaction intermediates, H−M$^+$−XH$_{n-1}$, whose existence is hypothesized by the experimentalists for the reaction of early and middle first-row transition metal cations were localized along the paths and characterized. Because of the excited nature of this intermediate with respect to the ground state of the reactants, the reactions are presumed to occur via a crossing from the high-spin to the low-spin surface.

The comparison between the surfaces for the reaction with ammonia and methane suggests that the donation of nitrogen lone pair into d orbitals of the metal is not operative in this case, due to the particularly stable 4s3d^5 configuration of the ground state. The same conclusion can be drawn considering the trend of binding energies for the products of the three exit channels of the insertion reaction for all the cations from Sc to Mn.

Work is in progress to perform analogous studies for the late first row transition metal cations.

References and Notes

(1) Freas, R. B.; Ridge, D. P. *J. Am. Chem. Soc.* **1980**, *102*, 7129.
(2) Aristov, A.; Armentrout, P. B. *J. Am. Chem. Soc.* **1984**, *106*, 4065.
(3) Tolbert, M. A.; Beauchamp, J. L. *J. Am. Chem. Soc.* **1984**, *106*, 8117.
(4) Reents, W. L.; Strobel, F.; Freas, R. B.; Wronka, J.; Ridge, D. P. *J. Phys. Chem.* **1985**, *89*, 5666.
(5) Aristov, N.; Armentrout, P. B. *J. Phys. Chem.* **1986**, *108*, 1806.
(6) Kang, N.; Beauchamp, J. L. *J. Am. Chem. Soc.* **1986**, *108*, 7502.
(7) Aristov, N.; Armentrout, P. B. *J. Phys. Chem.* **1987**, *91*, 6178.
(8) Sunderlin, L. S.; Armentrout, P. B. *J. Phys. Chem.* **1988**, *92*, 1209.
(9) Georgiadis, R.; Armentrout, P. B. *J. Phys. Chem.* **1988**, *92*, 7067.
(10) Tonkyn, R.; Ronan, M.; Weisshaar, J. C. *J. Phys. Chem.* **1988**, *92*, 92.
(11) Buckner, S. W.; Gord, J. R.; Freiser, B. S. *J. Am. Chem. Soc.* **1988**, *110*, 6606.
(12) Irikura, K. K.; Beauchamp, J. L. *J. Am. Chem. Soc.* **1989**, *111*, 75.
(13) Sunderlin, L. S.; Armentrout, P. B. *J. Am. Chem. Soc.* **1989**, *111*, 3845.
(14) Magnera, T. F.; David, D. E.; Michl, J. *J. Am. Chem. Soc.* **1989**, *111*, 4100.
(15) Armentrout, P. B.; Beauchamp, J. L. *Acc. Chem. Res.* **1989**, *22*, 315.
(16) *Gas-Phase Inorganic Chemistry*; Russel, D. H., Ed.; Plenum: New York, 1989; p 412.
(17) Armentrout, P. B. *Annu. Rev. Phys. Chem.* **1990**, *41*, 313.
(18) Clemmer, D. E.; Sunderlin, L. S.; Armentrout, P. B. *J. Phys. Chem.* **1990**, *94*, 208.
(19) Clemmer, D. E.; Sunderlin, L. S.; Armentrout, P. B. *J. Phys. Chem.* **1990**, *94*, 3008.
(20) Armentrout, P. B. *Science* **1991**, *41*, 175−179.
(21) Fisher, E. R.; Armentrout, P. B. *J. Am. Chem. Soc.* **1992**, *114*, 2049.
(22) Guo, B. C.; Kerns, K. P.; Castleman, A. W. *J. Phys. Chem.* **1992**, *96*, 4879.
(23) Clemmer, D. E.; Aristov, N.; Armentrout, P. B. *J. Phys. Chem.* **1993**, *97*, 544.
(24) Chen, Y.; Clemmer, D. E.; Armentrout, P. B. *J. Phys. Chem.* **1994**, *98*, 11 490.
(25) Chen, Y.; Armentrout, P. B. *J. Phys. Chem.* **1995**, *99*, 10 775.
(26) Haynes, C. L.; Chen, Y.; Armentrout, P. B. *J. Phys. Chem.* **1995**, *99*, 9110.
(27) Irigoras, A.; Fowler, J. E.; Ugalde, J. M. *J. Phys. Chem.* **1998**, *102*, 293.
(28) Irigoras, A.; Fowler, J. E.; Ugalde, J. M. *J. Am. Chem. Soc.* **1999**, *121*, 574.
(29) Irigoras, A.; Fowler, J. E.; Ugalde, J. M. *J. Am. Chem. Soc.* **1999**, *121*, 8549.
(30) Irigoras, A.; Elizalde, O.; Silanes, I.; Fowler, J. E.; Ugalde, J. M. *J. Am. Chem. Soc.* **2000**, *122*, 114.
(31) Abashkin, Y. G.; Burt, S. K.; Russo, N. *J. Phys. Chem.* **1997**, *101*, 8085.
(32) Russo, N.; Sicilia, E. *J. Am. Chem. Soc.* **2001**, *123*, 2588.
(33) Sicilia, E.; Russo, N. *J. Am. Chem. Soc.* **2002**, *124*, 1471.
(34) Bent, H. A. *J. Chem. Educ.* **1966**, *43*, 170.
(35) Schroder, D.; Shaik, S.; Bronstrup; Schwarz, H. *Acc. Chem. Res.* **2000**, *33*, 139.
(36) Bartlett, R. J. *Annu. Rev. Phys. Chem.* **1981**, *32*, 358.
(37) Raghavachari, K.; Trucks, G. W.; Pople, J. A.; Head-Gordon, M. *Chem. Phys. Lett.* **1989**, *157*, 479.
(38) Bauschlicher, C. W., Jr.; Ricca, A.; Partridge, H.; Scuseria, G. E. *J. Chem. Phys.* **1992**, *97*, 7471.
(39) Bauschlicher, C. W., Jr.; Ricca, A.; Partridge, H.; Langghoff, S. R. in *Recent Advances in Density Functional Theory*; Chong, D. P., Ed.; World Scientific Publishing Co.: Singapore, 1997; Part II and references therein.

(40) Halthausen, M. C.; Fiedler, A.; Schwarz, H.; Koch, W. *J. Phys. Chem.* **1996**, *100*, 6236.

(41) Thomas, J. L. C.; Bauschlicher, C. W., Jr.; Hall, M. B. *J. Phys. Chem.* **1997**, *101*, 8530.

(42) Sodupe, M.; Branchadell, V.; Rosi, M.; Bauschlicher, C. W., Jr. *J. Phys. Chem.* **1997**, *101*, 7854.

(43) Strobel, F.; Ridge, D. P. *J. Phys. Chem.* **1989**, *93*, 3635.

(44) Sunderlin, L. S.; Armentrout, P. B. *J. Phys. Chem.* **1990**, *94*, 3589.

(45) Derek, W.; Armentrout, P. B. *J. Am. Chem. Soc*. **1998**, *120*, 3176.

(46) Hendrickx, M.; Ceulemans, M.; Gong, K.; Vanquickenborne, L. *J. Phys. Chem.* **1997**, *101*, 2465.

(47) Tsipis, A. C. *J. Chem. Soc., Faraday Trans.* **1998**, *94*, 11.

(48) Langhoff, S. R.; Bauschlicher, C. W.; Partridge, H.; Sodupe, M. *J. Phys. Chem.* **1991**, *95*, 10 677.

(49) Becke, A. D. *J. Chem. Phys.* **1993**, *98*, 5648.

(50) Lee, C.; Yang, W.; Parr, R. G. *Phys. Rev. B* **1988**, *37*, 785.

(51) Godbout, N.; Salahub, D. R.; Andzelm, J.; Wimmer, E. *Can. J. Chem.* **1992**, *70*, 560.

(52) Davidson, E. R. *Chem. Rev.* **2000**, *100*, 351.

(53) Aschi, M.; Bronstrup, M.; Diefenbach, M.; Harvey, J. N.; Schroder, D.; Schwarz, H. *Angew. Chem., Int. Ed. Engl.* **1998**, *37*, 829.

(54) Yi, S. S.; Blomberg, M. R. A.; Siegbahn, P. E. M.; Weisshaar, M. *J. Phys. Chem.* **1998**, *102*, 395.

(55) Carpenter, J. E.; Weinhold, F. *J. Mol Struct. (THEOCHEM)* **1988**, *169*, 41.

(56) Carpenter, J. E.; Weinhold, F. J. *The Structure of Small Molecules and Ions*; Plenum: New York, 1988.

(57) Frisch, M. J.; Trucks, G. W.; Schlegel, H. B.; Gill, P. M. W.; Johnson, B. G.; Robb, M. A.; Cheesman, J. R.; Keith, T. A.; Petersson, G. A.; Montgomery, J. A.; Raghavachari, K.; Al-Laham, M. A.; Zakrzewski, V. G.; Ortiz, J. V.; Foresman, J. B.; Croslowski, J.; Stefanov, B. B.; Nanayakkara, A.; Challacombe, M.; Peng, C. Y.; Ayala, P. Y.; Chen, W.; Wong, M. W.; Andres, J. L:; Peplogle, E. S.; Gomperts, R.; Martin, R. L.; Fox, D. J.; Binkley, J. S.; Defrees, D. J.; Baker, J.; Stewart, J. P.; Head-Gordon, M.; Gonzales, C.; Pople, J. A. *Gaussian 94*, revision A.1; Gaussian, Inc.: Pittsburgh, PA, 1995.

(58) Moore, C. E. *Atomic Energy Levels*; NSRD-NBS, USA; U.S. Government Printing Office: Washington, DC, 1991; Vol 1.

(59) Elkind, J. L.; Armentrout, P. B. *J. Chem. Phys.* **1986**, *84*, 4862.

(60) Georgiadis, R.; Armentrout, P. B. *Int. J. Mass Spectrom. Ion Processes* **1989**, *91*, 123.

(61) Sunderlin, L. S.; Armentrout, P. B. *J. Phys. Chem.* **1990**, *94*, 3589.

(62) See for example: (a) Halthausen, M. C.; Heinemann, C.; Cornehl, H. H.; Koch, W.; Schwarz, H. *J. Chem. Phys.* **1995**, *102*, 4931. (b) Ricca, A.; Bauschlicher, C. W., Jr. *Chem. Phys. Lett.* **1995**, *245*, 150.

(63) Durant, J. L. *Chem Phys. Lett.* **1996**, *256*, 595.

(64) Jursic, B. S. *Chem Phys. Lett.* **1997**, *264*, 113.

(65) Basch, H.; Hoz, S. *J. Chem. Phys*. **1997**, *101*, 4416.

(66) Lynch, B. J.; Fast, P. L.; Harris, M.; Truhlar, D. G. *J. Phys. Chem. A* **2000**, *104*, 4811.

(67) Lynch, B. J.; Fast, P. L.; Harris, M.; Truhlar, D. G. *J. Phys. Chem. A* **2001**, *105*, 2936.

(68) Halthausen, M. C.; Koch, W. *J. Am. Chem. Soc*. **1996**, *118*, 9932.

(69) Elkind, J. L.; Sunderlin, L. S.; Armentrout, P. B. *J. Phys. Chem.* **1989**, *93*, 3151.

(70) Elkind, J. L.; Armentrout, P. B. *Int. J. Mass Spectrom. Ion Processes* **1988**, *83*, 258.

(71) Elkind, J. L.; Armentrout, P. B. *J. Chem. Phys.* **1987**, *86*, 1868.

(72) Sunderlin, L. S.; Armentrout, P. B. *Int. J. Mass Spectrom. Ion Processes* **1989**, *94*, 149.

(73) Georgiadis, R.; Armentrout, P. B. *Int. J. Mass Spectrom. Ion Processes* **1989**, *89*, 227.

(74) Armentrout, P. B. *ACS Symp. Ser.* **1990**, *4281*, 18.

(75) Armentrout, P. B.; Kickel, B. L. In *Organometallic Ion Chemistry*; Freiser, B. S., Ed.; Kluwer: Dordrecht, 1996.

(76) Schilling, J. B.; Goddard, W. A., III; Beauchamp, J. L. *J. Am. Chem. Soc*. **1986**, *108*, 582.

(77) Elkind, J. L.; Armentrout, P. B. *J. Phys. Chem.* **1987**, *91*, 2037.

(78) Carter, E. A.; Goddard, W. A. *J. Phys. Chem.* **1988**, *92*, 5689.

(79) Kapellos, S.; Mavridis, A.; Harrison, J. F. *J. Phys. Chem.* **1991**, *95*, 6860.